

Maximizing weighted Shannon entropy for network inference with little data

Danh-Tai Hoang,^{1,2} Juyong Song,^{3,4} Vipul Periwal,^{1,*} and Junghyo Jo^{3,4,†}

¹Laboratory of Biological Modeling, National Institute of Diabetes and Digestive and Kidney Diseases, National Institutes of Health, Bethesda, Maryland 20892, USA

²Department of Natural Sciences, Quang Binh University, Dong Hoi, Quang Binh 510000, Vietnam

³Asia Pacific Center for Theoretical Physics, Pohang, Gyeongbuk 37673, Korea

⁴Department of Physics, Pohang University of Science and Technology, Pohang, Gyeongbuk 37673, Korea

(Dated: May 6, 2022)

Experimental datasets for system inference often do not exhibit theoretical desiderata such as known and amenable distributions of couplings, and have no guarantee of sparse connectivity. An example is that of network reconstruction for brain networks with data from various imaging modalities. In this Letter, we introduce an entirely data-driven approach to model inference based on maximizing Shannon entropy using Schwinger's approach in the mathematical formalism of statistical physics and show model recovery in the limit of little data. Our self-consistent iterative algorithm can infer coupling strengths in non-equilibrium kinetic Ising models and outperforms previous approaches, particularly in the large coupling variability and little data regimes. Furthermore, the algorithm can be used to infer higher order interactions systematically, and the computation scales to larger systems as it is completely parallelizable.

Introduction. While Big Data is the zeitgeist, complex systems do not always afford enough data to allow complete system identification. Theorists contend with the computational difficulties of inferring large systems by positing properties such as sparsity of interactions or specifying distributions of couplings, usually with scant experimental support. Our experience is primarily in biological model inference [1, 2], where the complexity of living organisms engendered by the inherent stochasticity of the underlying processes of mutation and natural selection makes theoretical presumptions foolhardy, but similar system identification problems arise in many scientific areas [3, 4].

Network inference from large-scale brain/neuron activities at cellular resolution [5] is a challenging example of a non-equilibrium problem [6–8]. Regarding statistical physics as the answer to such problems is natural for physicists [9, 10], but in fact, especially for under-determined problems, system interactants are rarely interchangeable and the observed configurations of the system bear no semblance to random sampling or a putative thermodynamic limit. Our approach here is to utilize the powerful mathematical formalism of statistical physics to approach system inference in a principled way. We shall show that maximizing an appropriately weighted Shannon entropy is the same as minimizing a free energy function, and this maximization can be used iteratively to infer complex system interactions in stochastic systems.

Theory. For our purposes, the mathematical formalism of statistical physics in Schwinger's approach [11, 12] provides a natural connection between expectation values of microstates and expectation values of observables of microstates. Define a generating function computed from the observed spin configurations: $Z_h(J) = \sum_t \exp(J \cdot \sigma(t) - \beta h(t))$, where $h(t)$ is some observed characteristic of a spin configuration $\sigma(t)$, and β is a conjugate 'inverse temperature' variable. A free energy, $F_h = \log Z_h$, can be used to calculate expectation values of

spin activities,

$$\frac{\partial F_h}{\partial J_i} = \frac{\sum_t \sigma_i(t) \exp(J \cdot \sigma(t) - \beta h(t))}{\sum_t \exp(J \cdot \sigma(t) - \beta h(t))} = \langle \sigma_i \rangle_J \equiv m_i(J). \quad (1)$$

Here J is an inhomogeneous magnetic field, a vector of time-independent variables J_i for each spin σ_i , so we interpret $m_i(J)$ as the induced magnetization of spin σ_i . Varying J leads to changes in the vector of magnetizations $m(J)$. Each term in the partition sum is treated as an independent observation, and the order implicit in the time-series is clearly irrelevant. Naïvely, each possible microstate of the N spins is an attainable value of $m(J)$, but this is false as we sum over observed configurations of spins only and there is no assumption of summing over a complete set of configurations, nor of random sampling. With a Legendre transform, m becomes the independent variable, and $J(m)$ the dependent variable:

$$F_h(J) + G_h(m) = J \cdot m. \quad (2)$$

The duality relation between F_h and G_h gives

$$\frac{\partial G_h}{\partial m_i} = J_i(m). \quad (3)$$

The free energy $G_h(m)$ can be interpreted as the negative of the Shannon entropy for data with the assignment of likelihoods $\exp(J(m) \cdot \sigma(t))$, and normalizing to get probabilities: $1 = \sum_t' \exp(J(m) \cdot (\sigma(t) - m) + G_h) \equiv \sum_t' p_t$, where $\sum_t' \equiv \sum_t \exp(-\beta h(t))$, with the weight factor $\exp(-\beta h(t))$ in the summation similar to the appearance of weights in noncentral hypergeometric distributions. Defining the weighted Shannon entropy, $S(m) \equiv -\sum_t' p_t \ln p_t$, we have $S = \sum_t' p_t (-J(m) \cdot (\sigma(t) - m) - G_h) = -G_h$ using $m = \langle \sigma \rangle_{J(m)}$. Thus minimizing $G_h(m)$ with respect to m is equivalent to maximizing this Shannon entropy of the weighted data.

The expectation value of h is obtained by differentiation,

$$\frac{\partial G_h}{\partial \beta} = -\frac{\partial F_h}{\partial \beta} = \frac{\sum_t h(t) \exp(J \cdot \sigma(t) - \beta h(t))}{\sum_t \exp(J \cdot \sigma(t) - \beta h(t))} = \langle h \rangle_{J(m)}. \quad (4)$$

Therefore, if one knows the free energy $G_h(m)$ as a function of β , one has a map: $m \mapsto \langle h \rangle_{J(m)}$, which provides the advertised connection between a microstate and the expected value of an observable for that microstate. We can expand $G_h(m)$ near a chosen m^* , with $J^* \equiv J(m^*)$, by using its Taylor series up to the second term,

$$G_h(m) = G_h(m^*) + J^* \cdot (m - m^*) + \frac{1}{2}(m - m^*) \cdot K^* \cdot (m - m^*)^T, \quad (5)$$

where J^* and K^* are the first and second derivatives at m^* . K is the inverse covariance matrix:

$$\begin{aligned} K_{ij}^{-1} &= \left[\frac{\partial^2 G_h}{\partial m_i \partial m_j} \right]^{-1} = \left[\frac{\partial J_j}{\partial m_i} \right]^{-1} \\ &= \frac{\partial m_i}{\partial J_j} = \frac{\partial^2 F_h}{\partial J_i \partial J_j} = \langle \sigma_i \sigma_j \rangle_{c,J}. \end{aligned} \quad (6)$$

where the subscript c denotes the connected correlation function. An advantage of Schwinger's formulation [11, 12] is that possible higher order interactions are consistently incorporated by continuing Eq. (5) to higher orders in derivatives. Even if $G_h(m)$ cannot be computed for all microstates by picking the appropriate value of $J(m)$ given available data, Eq. (5) contains system coupling information.

We fix $J^* = 0$ as this will maximize the Shannon entropy. Differentiating Eq. (5) with respect to β gives

$$\frac{\partial G_h(m)}{\partial \beta} = \frac{\partial G_h(m^*)}{\partial \beta} - \sum_{i,j=1}^N K_{ij}^* \frac{\partial m_i^*}{\partial \beta} (m_j - m_j^*), \quad (7)$$

where $\partial m_i^* / \partial \beta = -\langle h \sigma_i \rangle_{c,J^*}$. Up to linear order, we have

$$\langle h \rangle_{J(m)} = \langle h \rangle_{J^*} + \sum_{i,j=1}^N \langle \sigma_i \sigma_j \rangle_{c,J^*}^{-1} \langle h \sigma_i \rangle_{c,J^*} (m_j - m_j^*). \quad (8)$$

To be specific, consider the kinetic Ising model which has N spins taking values ± 1 that are stochastically updated with the following parametrized conditional probability:

$$P(\sigma_i(t+1)|\sigma(t)) = \frac{\exp(\sigma_i(t+1)H_i(t))}{\exp(H_i(t)) + \exp(-H_i(t))}, \quad (9)$$

where $H_i(t) \equiv \sum_j W_{ij} \sigma_j(t)$, and $E(\sigma_i(t+1)) = \tanh H_i(t)$, where $E(\cdot)$ is the expectation value using the distribution in Eq. (9). Given a time sequence of spin configurations, $\sigma(t) = (\sigma_1, \sigma_2, \dots, \sigma_N)$, $t \in \{1, \dots, L\}$, our goal is to infer the connection weights W_{ij} . The standard Maximum A Posteriori (MAP) estimate of the connection weights maximizes $\mathcal{P} = \prod_{t=1}^{L-1} \prod_{i=1}^N P(\sigma_i(t+1)|\sigma(t))$, with respect to W_{ij} to determine the weights. By construction, the MAP estimate converges to the true probabilities in the large L limit.

We define an expectation value $E_i(\cdot)$ of functions of spin configurations as follows:

$$E_i(f) = \frac{\sum_t \sigma_i(t+1) f(\sigma(t)) \exp(J \cdot \sigma(t) - \beta h(t))}{\sum_t \exp(J \cdot \sigma(t) - \beta h(t))}. \quad (10)$$

The sum in the numerator can be separated as

$$\begin{aligned} &\sum_{\sigma(t): \sigma_k(t+1)=+1} f(\sigma(t)) \exp(J \cdot \sigma(t) - \beta h(t)) \\ &- \sum_{\sigma(t): \sigma_k(t+1)=-1} f(\sigma(t)) \exp(J \cdot \sigma(t) - \beta h(t)), \end{aligned} \quad (11)$$

but in the kinetic Ising model the probability of a configuration $\sigma(t)$ falling into the first or the second sums can be combined to give

$$E_i(f) \approx \frac{\sum_t \tanh(H_i(t)) f(\sigma(t)) \exp(J \cdot \sigma(t) - \beta h(t))}{\sum_t \exp(J \cdot \sigma(t) - \beta h(t))}, \quad (12)$$

as an approximation to the actual finite observed sum. This observation is completely independent of the choice of f or h . In particular, we get

$$\langle \sigma_i(t+1) f(t) \rangle_J \equiv E_i(f(t)) \approx \langle \tanh(H_i(t)) f(t) \rangle_J. \quad (13)$$

If we redefine

$$h(t) \rightarrow h_i(t) \equiv \sigma_i(t+1) \frac{H_i(t)}{\tanh(H_i(t))}, \quad (14)$$

we obtain $\langle h_i(t) \sigma_j(t) \rangle_J \approx \langle H_i(t) \sigma_j(t) \rangle_J$. As $H_i(t) = \sum_j W_{ij} \sigma_j(t)$ in the kinetic Ising model, with a finite amount of data and starting from a randomly chosen $W_{ij} \mapsto H_i(t)$, we can define $h_i(t)$ using Eq. (14) and then use Eq. (13) to update the value of W_{ij} with Eq. (8), working on one spin index i at a time. To find the 'true' W_{ij} , we repeat the iteration of $W_{ij} \mapsto H_i(t) \mapsto h_i(t) \mapsto \langle h_i(t) \rangle \mapsto W_{ij}$.

Results. Inference in under-determined problems must include some criterion to avoid over-fitting. We first developed a procedure for the case studied in the literature [13, 14] of normally distributed W_{ij} with variance g^2/N and mean zero. The accuracy of inference is estimated using the mean square error:

$$\text{MSE} = \frac{1}{N^2} \sum_{i,j=1}^N (W_{ij} - W_{ij}^{\text{true}})^2. \quad (15)$$

When we infer W_{ij} in our iteration, we stop updates if the change is less than a predefined threshold ($\delta W_{ij} < \Delta$). In the limit of a large number of observed configurations and weak coupling variability (large L/N and small g), MSE decreases and saturates as Δ decreases (Fig. 1a). Therefore, the choice of Δ is immaterial in this limit so long as it is small enough. In the limit of few observed configurations and strong coupling variability (small L/N and large g), however, MSE is a nontrivial function of Δ , and too small Δ leads to over-fitting and erroneous inference (Fig. 1b).

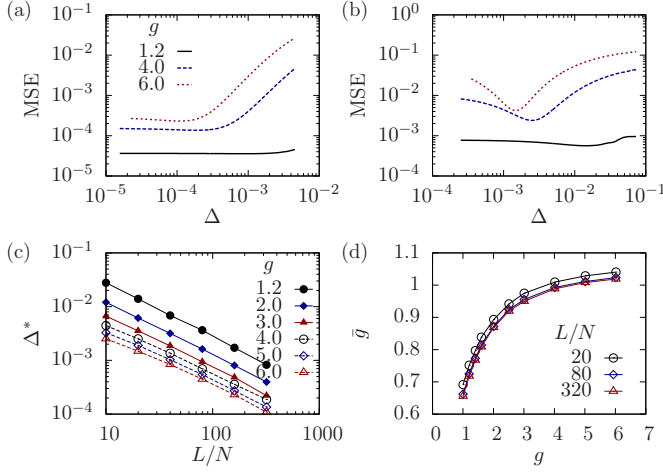


FIG. 1. (Color online) Inference accuracy depending on parameter values and problems. Mean square error (MSE) of inferred coupling strengths W_{ij} depends on the threshold Δ for stopping the iteration ($\delta W_{ij} < \Delta$), given (a) large ($L/N = 320$) and (b) small ($L/N = 20$) numbers of observed configurations with a system size ($N = 200$). Different variances of true coupling strengths (g^2/N) are considered. (c) Optimal thresholds Δ^* for minimal MSE and (d) effective coupling variability \bar{g} , estimated from the data correlation $\langle \sigma_i(t+1)\sigma_j(t) \rangle_c$, depend on the data length L/N and coupling strength g .

We hypothesized that a systematic dependence of the optimal value Δ^* on L , N , and g would lead to the lowest MSE attainable. First we found that Δ^* decreases when L/N and/or g increase(s) (Fig. 1c). W_{ij} is unknown so the coupling variability g cannot be estimated. We introduced an observable effective coupling variability $\bar{g} = s\sqrt{N}$ where s is the standard deviation of the distribution of the observed $\langle \sigma_i(t+1)\sigma_j(t) \rangle_c$ values. When g increases, \bar{g} increases strongly at small g but slowly at large g (Fig. 1d). The two scale relations guided us to write $\Delta^*(L, N, \bar{g}) = (L/N)^{-1}f(N, \bar{g})$, where $f(N, \bar{g}) = u(N)(\bar{g}^{-2} - b)$ is fitted with $u(N) = a_0 + a_1\sqrt{N}^{-1}$ with $a_0 = 0.074 \pm 0.005$, $a_1 = 2.791 \pm 0.070$, and $b = 0.805 \pm 0.003$ (Figs. 2a-c). Interestingly, $b \approx \bar{g}_{\max}^{-2}$ where \bar{g}_{\max} represents the saturation value of \bar{g} (Fig. 1d). Therefore, we obtain the optimal threshold:

$$\Delta^* = \left(\frac{L}{N}\right)^{-1} \left(a_0 + \frac{a_1}{\sqrt{N}}\right) \left(\frac{1}{\bar{g}^2} - \frac{1}{\bar{g}_{\max}^2}\right). \quad (16)$$

Using this criteria, we inferred the coupling strengths and compared the performance of our approach with gradient descent MAP inference. In the limit of weak coupling variability ($g = 1.2$) and a large number of observed configurations ($L/N = 160, 320$), our method works as well as MAP. However, in the limit of strong coupling variability ($g = 4.0, 6.0$) and/or smaller numbers of observed configurations ($L/N = 10, 20$), our method provided much better accuracy (Fig. 2d). For $L/N = 10$ and $g = 6.0$, MSE obtained using our method is approximately 4 times lower than that using MAP inference.

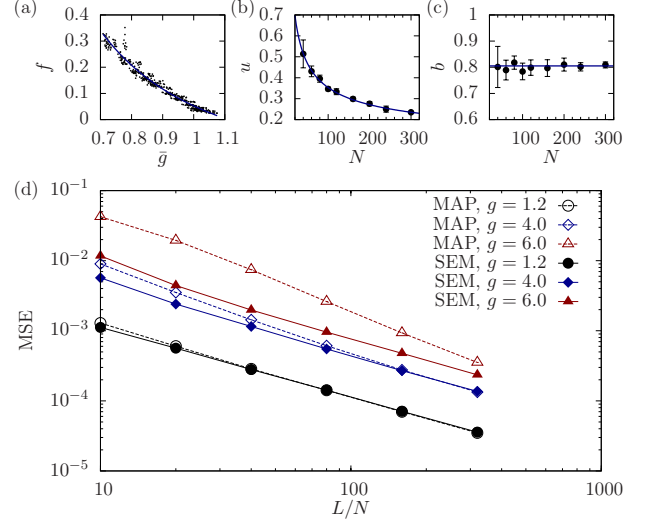


FIG. 2. (Color online) Accurate inference for normally-distributed couplings. (a) $f(N, \bar{g})$ inversely varies with the effective variability \bar{g} given a fixed system size ($N = 200$). Black dots represent 500 ensembles generated from different trials with various data lengths ($L/N = [10, 160]$) and coupling strengths ($g = [1.2, 6]$). The fitting line represents $f(N, \bar{g}) = u(\bar{g}^{-2} - b)$ with $u = 0.276$ and $b = 0.810$. The fitting parameter (b) u depends on the system size N , while (c) b does not depend on N . Their values are obtained from ensemble averages of 10 different trials, of which standard deviations give the error bars. Here the fitting lines represent (b) $u = a_0 + a_1\sqrt{N}^{-1}$ with $a_0 = 0.074$ and $a_1 = 2.791$, and (c) $b = 0.805$ independent on N . (d) Mean square errors of inferred coupling strengths are obtained from our method (solid lines), based on the Shannon Entropy Maximization (SEM), and from the standard gradient descent method (dotted lines), based on Maximum A Posteriori (MAP), for various coupling strengths.

We want an entirely data-driven approach but Eq. (16) is specific to normally distributed couplings. To quantify the predictability of $\sigma_i(t+1)$ from $H_i(t)$, we measure the discrepancy between $\sigma_i(t+1)$ and its expectation, $E(\sigma_i(t+1)) = \tanh(H_i(t))$, as a cost for each spin i ,

$$C_i(W_{ij}) \equiv \sum_t [\sigma_i(t+1) - \tanh(H_i(t))]^2, \quad (17)$$

where $H_i(t) = \sum_j W_{ij}\sigma_j(t)$. The cost can be rewritten as $C_i(W_{ij}) = \sum_t [\sigma_i(t+1) - \sigma_i(t+1)P(\sigma_i(t+1)|\sigma(t))]^2 = \sum_t [1 - P(\sigma_i(t+1)|\sigma(t))]^2$ with the transition probability, $P(\sigma_i(t+1)|\sigma(t))$ in Eq. (9). Thus the cost decreases as W_{ij} predicts transitions better. We found that the minimization of this cost provides a suitable iteration stopping criterion for general distributions of couplings. We show two examples of inferred networks. In the first example, the spins have alternating bands of positive and negative couplings modulated by distance as $|W_{ij}| = W_0/\log(R_{ij})$, where R_{ij} represents the radius of the circle. The spin raster scan exhibits nontrivial structure (Fig. 3a), reminiscent of binocular rivalry [15]. As the number of observed configurations increases, the predicted coupling strengths (Figs. 3b-d) approach their true val-

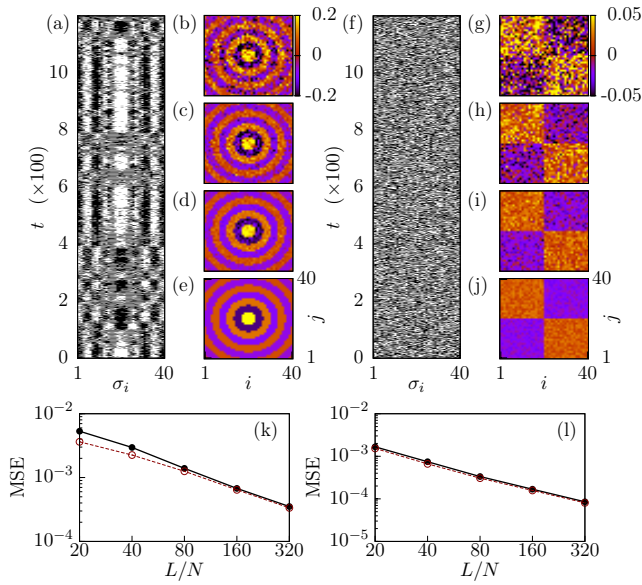


FIG. 3. (Color online) Effectiveness of data-driven stopping rule. Given $N = 40$ spin variables, (a, f) typical time-series of their activities are plotted for band and block structures of positive and negative coupling strengths depending on sites. Predicted coupling weights are plotted for different data lengths (b, g) $L = 800$, (c, h) 3200, (d, i) 12800, and (e, j) true coupling weights are also plotted. Mean square errors (MSE) of the prediction are obtained for using the data-driven stopping rule (black lines), which are compared with the real MSE minima (red lines) for (k) band and (l) block structure cases.

ues (Fig. 3e). In the second, the spins are in blocks of positive and negative couplings with no obvious structure in the simulated spin raster scan (Fig. 3f) but the coupling strengths (Figs. 3g-j) are still predicted well. The MSE obtained by using an increase in $C_i(W_{ij})$ as the stopping criterion is close to the actual minimum MSE over arbitrary numbers of iterations in either example (Figs. 3k and 3l).

Can the systematic Taylor expansion in Eq. (7) be used to infer nonlinear forms of $H_i(t)$? We simulated a network with quadratic couplings $H_i(t) = \sum_j W_{ij}\sigma_j(t) + \sum_{j,k} Q_{ijk}\sigma_j(t)\sigma_k(t)$, where W_{ij} and Q_{ijk} are normally distributed. The quadratic couplings are symmetric ($Q_{ijk} = Q_{ikj}$) and have no self-interactions ($Q_{ijj} = 0$) since $\sigma_j^2 = 1$. The number of Q_{ijk} parameters is $N^2(N-1)/2$. As shown in Fig. 4, our approach can recover nonlinear interactions, with no change in the computation, by simply expanding Eq. (7) up to a higher order: $\langle h \rangle_J = -(\partial_\beta m^* \cdot K^* + m^* \cdot \partial_\beta K^*) \cdot m^T + m \cdot \partial_\beta K^* \cdot m^T / 2$.

Conclusion. Our approach to solving the inference problem was to find a link via the Shannon entropy between states and their transition probabilities. Using the physical and mathematical underpinnings of statistical physics in Schwinger's formulation [11, 12], we ignored the MAP criterion. The usual approach in the literature [13] maximizes the MAP criterion by gradient descent with a learning rate α , $\delta W_{ij} = \alpha \partial \log \mathcal{P} / \partial W_{ij} = \alpha \sum_{t=1}^{L-1} (\sigma_i(t+1) - \tanh(H_i(t))) \sigma_j(t)$.

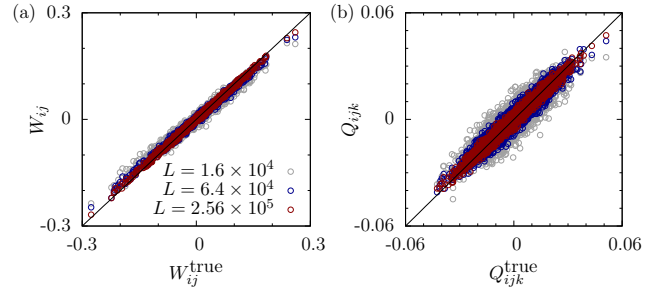


FIG. 4. (Color online) Accurate inference of higher-order coupling strengths. (a) Linear and (b) quadratic coupling strengths in the nonlinear kinetic Ising model with the local field, $H_i(t) = \sum_j W_{ij}\sigma_j(t) + \sum_{j,k} Q_{ijk}\sigma_j(t)\sigma_k(t)$, are predicted from our method. Here the true coupling strengths are normally distributed with a system size ($N = 40$). Three different data lengths, $L = 1.6 \times 10^4$ (gray), 6.4×10^4 (blue) and 2.56×10^5 (red), are examined.

This is computationally expensive and tuning learning rates is an art, so other methods have been developed. The naïve mean field method requires the vanishing of the MAP gradient, which is a special case of Eq. (13), but it only works for weak coupling regimes ($g < 1$) [14].

Our algorithm applies to stochastic systems with an arbitrary number of discrete states. Computing spin by spin, it is embarrassingly parallelizable and assumes no symmetry in interactions between spins. The self-consistent iteration update based on Eq. (14) is a new way to solve the normalization constraint for probabilities. Our approach does not update connection weights incrementally so there is no learning parameter to tune. For under-determined systems, we gave a simple data-driven criterion for stopping learning in terms of the cost function $C_i(W_{ij})$ in Eq. (17). We exhibited the scalability of our method by applying it to systems with up to 300 interacting spins. While being able to use little data to make accurate inferences is obviously useful, another important aspect of inference with little data is that longer time-scale modulation of couplings can be inferred using a moving window. In conclusion, we have shown in this Letter that underdetermined stochastic systems can be inferred in a conceptually simple and computationally efficient manner using the maximization of the Shannon entropy in the mathematical framework of statistical physics.

This work was supported by Intramural Research Program of the National Institutes of Health, NIDDK (D.-T.H., V.P.), and by Basic Science Research Program through the National Research Foundation of Korea (NRF) funded by the Ministry of Education (2016R1D1A1B03932264) and the Max Planck Society, Gyeongsangbuk-Do and Pohang City (J.J.).

* vipulp@mail.nih.gov

† jojunghyo@apctp.org

- [1] J. P. Nguyen, F. B. Shipley, A. N. Linder, G. S. Plummer, M. Liu, S. U. Setru, J. W. Shaevitz, and A. M. Leifer, *Proc Natl Acad Sci U S A* **113**, E1074 (2016).
- [2] D. Bernal-Casas, H. J. Lee, A. J. Weitz, and J. H. Lee, *Neuron* **93**, 522 (2017).
- [3] M. Schmidt and H. Lipson, *Science* **324**, 81 (2009).
- [4] S. L. Brunton, J. L. Proctor, and J. N. Kutz, *Proc Natl Acad Sci U S A* **113**, 3932 (2016).
- [5] D. A. Dombeck, A. N. Khabbaz, F. Collman, T. L. Adelman, and D. W. Tank, *Neuron* **56**, 43 (2007).
- [6] E. Schneidman, M. J. Berry, 2nd, R. Segev, and W. Bialek, *Nature* **440**, 1007 (2006).
- [7] T. Watanabe, S. Hirose, H. Wada, Y. Imai, T. Machida, I. Shirouzu, S. Konishi, Y. Miyashita, and N. Masuda, *Nat Commun* **4**, 1370 (2013).
- [8] Y. Roudi, B. Dunn, and J. Hertz, *Curr Opin Neurobiol* **32**, 38 (2015).
- [9] J. Sohl-Dickstein, P. B. Battaglino, and M. R. DeWeese, *Phys Rev Lett* **107**, 220601 (2011).
- [10] A. Decelle and F. Ricci-Tersenghi, *Phys Rev Lett* **112**, 070603 (2014).
- [11] J. Schwinger, *The London, Edinburgh, and Dublin Philosophical Magazine and Journal of Science* **44**, 1171 (1953).
- [12] D. J. Toms, *The Schwinger action principle and effective action* (Cambridge University Press, 2007).
- [13] H.-L. Zeng, M. Alava, E. Aurell, J. Hertz, and Y. Roudi, *Phys Rev Lett* **110**, 210601 (2013).
- [14] Y. Roudi and J. Hertz, *Phys Rev Lett* **106**, 048702 (2011).
- [15] R. Moreno-Bote, J. Rinzel, and N. Rubin, *Journal of Neurophysiology* **98**, 1125 (2007).